

The Interaction of Ballistic Shock Waves with High-Speed Helium Jets

S.-L. HALL

Lecturer in Mechanical Engineering, New South Wales Institute Technology

SUMMARY Interaction pressure signatures and schlieren photographs were obtained with either of two rectangular nozzles having exit Mach numbers of 1.00 and 1.82 when delivering correctly-expanded helium jets. These nozzles were operated from 40 to 150% expansion at a fixed position (0.18m) relative to the pressure transducer; the trajectory of the 7.62mm projectile was either 36 or 108 body diameters from the transducer. All 422 interaction pressure signatures exhibited similar variety of waveforms as fighter and bomber aircraft. The wide variation in overpressure, rise time, duration and wave shape are attributed to the velocity and density fluctuations of the turbulent jets. Optical photographs show that the bow shock was always folded or wrinkled after passing through either of the jets. The tail shock experienced greater "bulging" and subsequent weakening in shock strength than the bow shock.

1 INTRODUCTION

All vehicles travelling supersonically create a system of pressure disturbances which causes sonic boom. The disturbances propagate through the atmosphere by waves radiating from the vehicle. The wave system ultimately forms an N-shaped pressure signature which manifests itself on the ground as two sharp, thunderous 'claps'.

In actual flight test measurements, the classic N-wave is rarely encountered. There are three main differences between pressure signatures measured in the real atmosphere and the classic N-wave: (1) there are random perturbations from the predicted wave shape; (2) shock rise times to peak overpressure of several milliseconds occur where the order of microseconds would be predicted for a quiescent atmosphere; and (3) there are variations in overall wave strength from point-to-point for a single flyover.

2 THEORETICAL MODELS

Several theories have been proposed since 1968 to explain one or more of the above signature distortion features.

2.1 Spiked and Rounded Waveforms

Generally, the spread of overpressure values vary little with aircraft type, decrease with increasing Mach number, and increase with temperature and with lateral distance from the flight path. It is widely concluded that this variability is caused by atmospheric perturbation, particularly turbulence.

Pierce (1968) proposed that atmospheric refraction would cause acoustic rays to be curved as they propagate through the inhomogeneous medium. Ripples which are concave outwards result in defocusing; those that are concave inwards result in focusing. The very narrow width of spikes were attributed to the loss of the lower frequency portion of the pressure signature by diffraction. A combination of nonlinear effects and finite rise time serve to limit the magnitude of peak overpressure.

Crow (1969) incorporated both thermal and inertial interaction in his first-order scattering theory. His theory has given quantitative predictions of waveform distortions. George and Plotkin (1971) superimposed a second-order perturbation on Crow's theory which attributes shock thickening to the turbulent scattering of the high frequency wave components. Maestrello et al (1974) propose that scattering redistributes acoustic energy in conjunction with convection and refraction effects.

Recently, Brown and Clifford (1976) have presented the viewpoint that turbulence broadens finite bands of sound, thereby causing attenuation.

2.2 Anomalous Rise Times

Turbulence is also held responsible for the experimentally observed randomness in rise times. Pierce (1971) extended the theory of geometric acoustics to predict a folded-shock structure. This mechanism would reduce the bow shock to a number of discrete pressure jumps or 'microshocks'. George and Plotkin (1971) proposed that nonlinear effects dominate in the creation of finite rise times. The equilibrium value would be governed by the signature overpressure and the state of turbulence in the atmosphere such that nonlinear steepening of the wave front will partly or totally offset the wave scattering process.

3 BALLISTIC LABORATORY INVESTIGATIONS

3.1 Optical Evidence of Shock-Distortion

3.1.1 Turbulent Wall Jet-Shock Interaction

The first evidence of 'wrinkled' shock fronts occurred in the shadowgraphs taken by Bauer and Bagley (1970) of ballistic shocks propagating through low-speed turbulent wall jets. The bow and tail shocks were broken into a number of lines by the interaction with the jets. Bauer and Bagley interpreted these lines as ripples in a smoothly-connected shock front. George (1970) attributes the multiple lines to lagging scattered waves; while Pierce and Maglieri (1972) believe that the shock fronts are multifolded.

3.1.2 Firing into a Variable Sound-Speed Gaseous Medium

More recently, the ballistic experiments of Sanai et al (1976) have produced schlieren photographs of fold-like shock structure for weak shocks and concave shock fronts for strong shocks.

3.1.3 Turbulent Free Jet-Shock Interaction

The results of the experiment described briefly in the SUMMARY are contained in Hall (1976). The optical photographs obtained are unambiguous in comparison with those from the above ballistic experiments. The shocks are always folded or wrinkled after passing through either of the helium jets. The Mach 1.8 nozzle was operated from 35% to 114% expansion; the Mach 1.0 nozzle was operated from 52% to 145% expansion.

Figure 1 shows a schlieren photograph of a 0.30 calibre projectile (Mach 2.5) and its wave system. Figures 2-5 present shock interaction photographs with the Mach 1.0 nozzle operating at 116, 100, 75, and 52% of the correct-expansion pressure ratio.

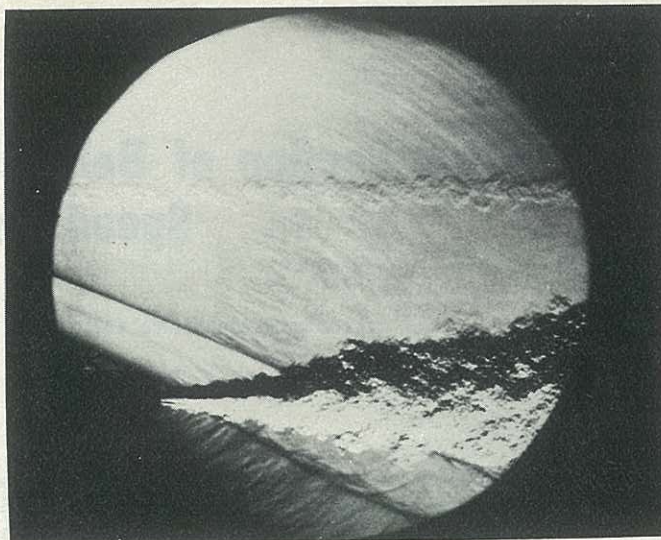


Figure 3 Mach 1.0 nozzle at 100% expansion
(Exit Mach no. = 1.003)

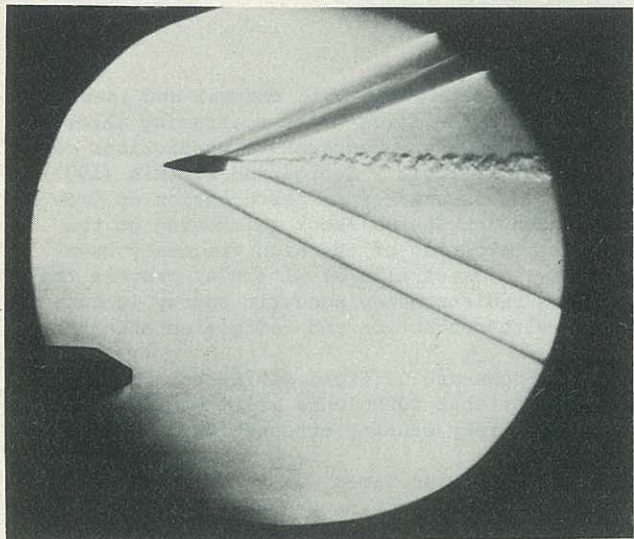


Figure 1 A 7.62mm NATO projectile
(Trajectory 98.4mm from nozzle centreline)

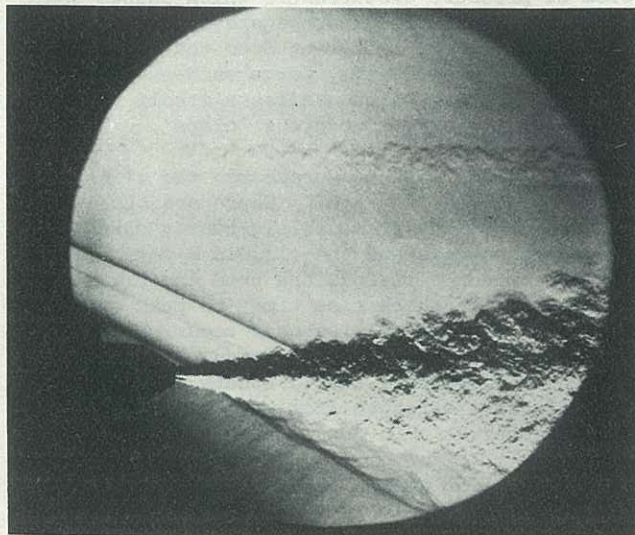


Figure 4 Mach 1.0 nozzle at 75% expansion
(Exit Mach no. = 0.755)

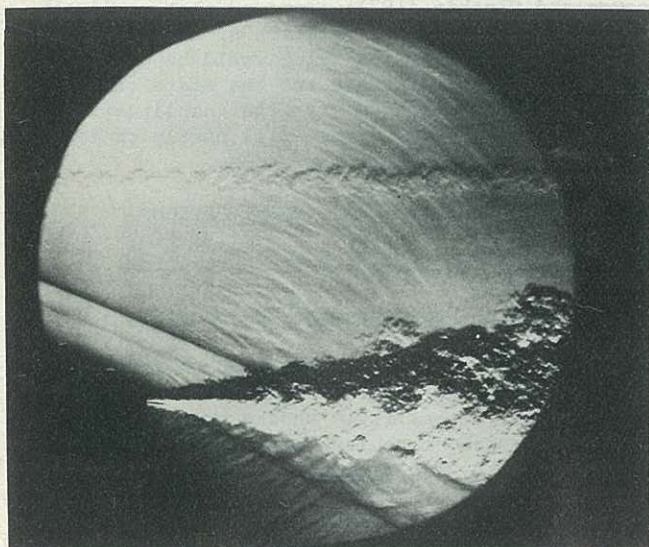


Figure 2 Mach 1.0 nozzle at 116% expansion
(Exit Mach no. = 1.117)

The overblown and the correctly-expanded Mach 1.0 jets have a close acoustic 'grid', indicating high frequency jet noise, and small-scale folding. The underblown jets have large-scale folding. Dr G.L. Brown (1975) observed that the size of the shock folding appears to correspond to the large instability wave pattern along the jet centreline. For the Mach 1.0 nozzle, the velocity of the large structure appears relatively high in comparison with the sound speed in the external flow, giving very large compressibility effects. The experimental work of Brown (1976), which varies Mach number and density independently, shows compressibility effects down to Mach 0.7.

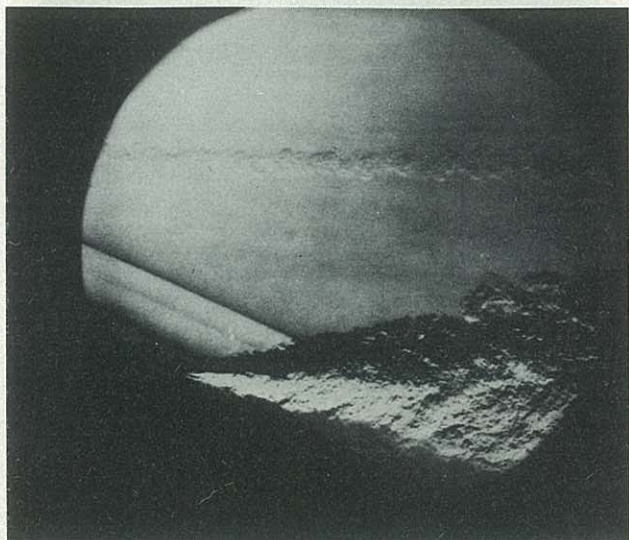


Figure 5 Mach 1.0 nozzle at 52% expansion
(Exit Mach no. = 0.283)

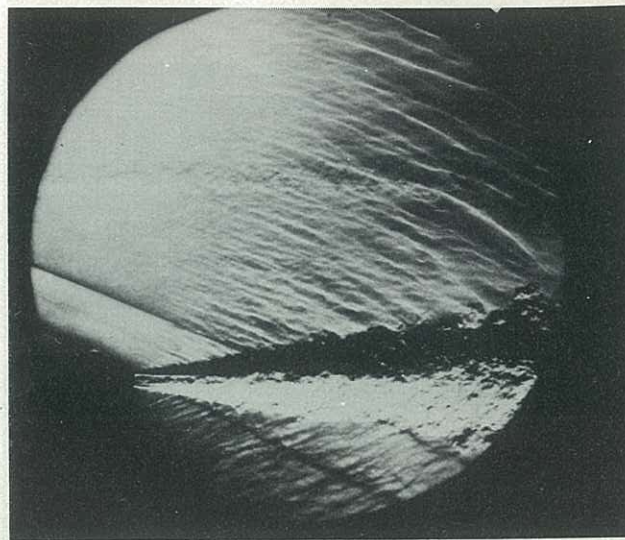


Figure 6 Mach 1.8 nozzle at 114% expansion
(Exit Mach no. = 1.917)

It is interesting to note there is no visible noise radiation from the 75% expansion jet before the pressure signature has passed through it; but there are closely-spaced (high frequency) curved waves on the 'underside' of the jet. It is obvious from Figure 5 that jet noise has no effect on the shock folding. There is no visible noise for the 52% expansion jet, but there is folding on the entire surface of the leading Mach core. Note that the bow shock appears to be broken-up (microshocks?) in the lower right-hand corner of the photograph.

Over the entire operating range of the Mach 1.0 nozzle, the 'wrinkled' shock fronts appear as a series of arcs originating from sources along the jet centreline. The radius of curvature for a given arc is roughly one-half the distance of the apparent centreline source from the nozzle exit.

The overlay of the jet noise pattern tends to obscure the 'wrinkling' near the jet, particularly for the Mach 1.8 nozzle interaction photographs. The greater intensity of the turbulence tends to refract and focus the distorted shock front as a relatively composite unit. Figures 6-8 indicate a high variability in local sound speed for the Mach 1.8 jets. The lightness and skewness of the tail shock after emerging from the jet (Figures 6 and 7) indicates a subsequent weakening in shock strength. It appears that the intensity of the acoustic field is about the same order of magnitude as the tail shock in these cases. The turbulence has decreased sufficiently for the 49% expansion jet to have a pattern similar to the series of arcs evident in all the Mach 1.0 interaction photographs.

As exit Mach number decreased, the size of the shock-front folds, as well as the divergent jet shear layer, increase and the shocks become increasingly bent forward by the jet. The tail shock shows greater bulging or deviation from a straight line than the bow shock. It would encounter a larger magnitude of turbulence due to the jet mixing increasing with distance from the nozzle exit.

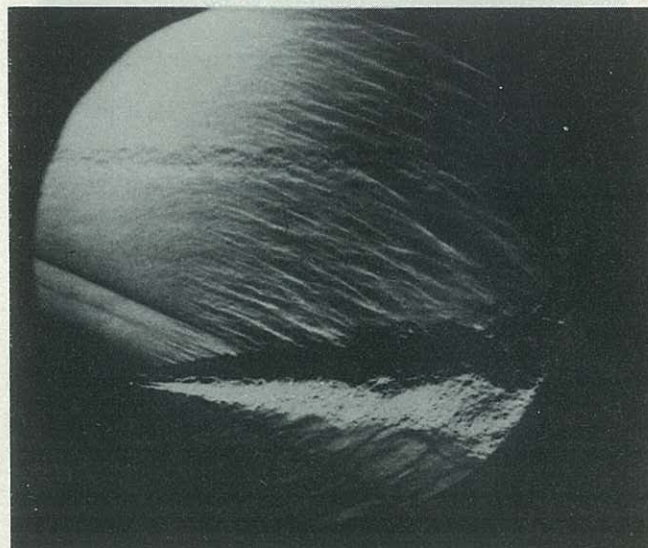


Figure 7 Mach 1.8 nozzle at 100% expansion
(Exit Mach no. = 1.820)

3.2 Interaction Pressure Signatures

All pressure signatures obtained with a helium jet operating exhibited similar varieties of waveforms as Lightning, F-104, B-58, XB-70, SR-71 and Concorde 002 flight test results. Examples of this variability may be seen in Figures 9-11; all pressure signatures have an amplitude of 1.57 kPa cm^{-1} , a sweep speed of $20 \mu \text{ sec cm}^{-1}$, a time delay of 2.025m sec, and an ambient pressure of 102 kPa. Signatures of the projectile only (no jet) and the jet only at 100% expansion are shown in Figures 9 and 10, respectively. Figures 11(a)-(c) are all shock-jet interaction photographs at 100% expansion. The signature shapes vary considerably, although all three shock-jet photographs have double positive-pressure peaks. Figure 11(b) looks like a rounded N-wave, while Figure 11(a) looks like the result

of a large amplitude jet being superimposed on the basic projectile N-wave.



Figure 8 Mach 1.8 nozzle at 49% expansion
(Exit Mach no. = 1.326)

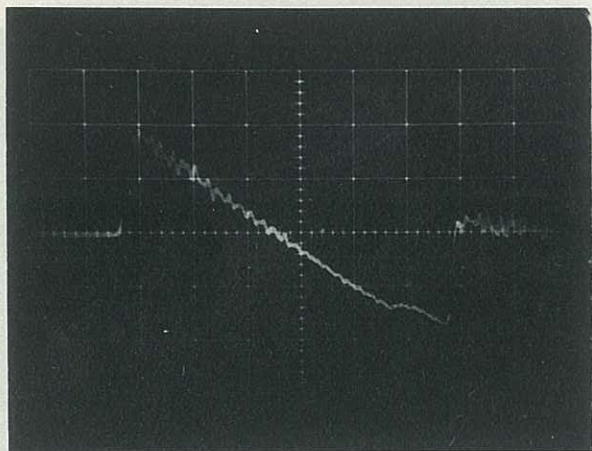


Figure 9 Projectile only pressure signature
(Trajectory 0.85m from transducer)

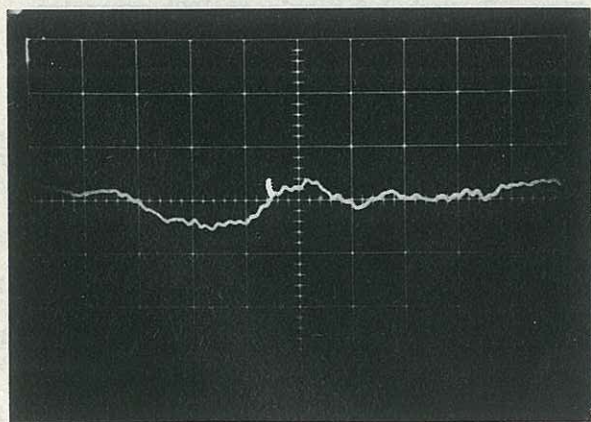
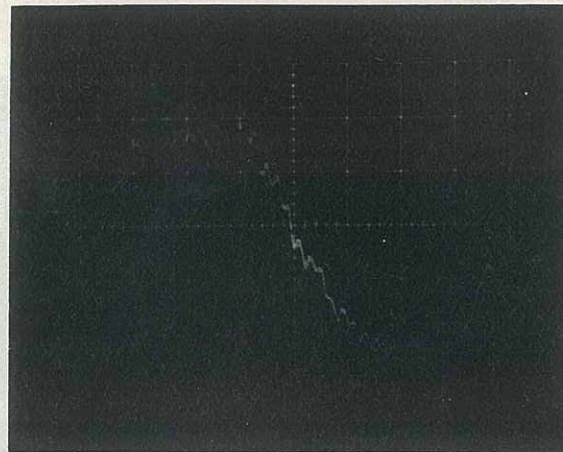
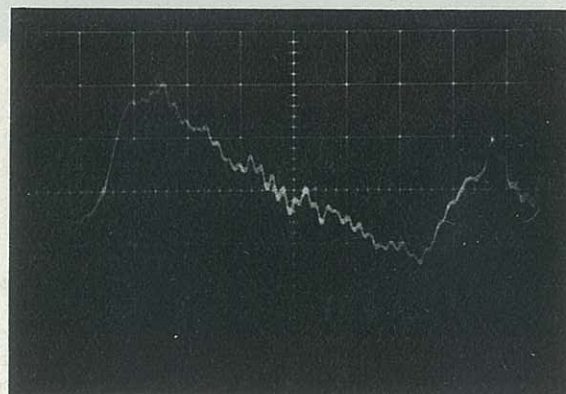


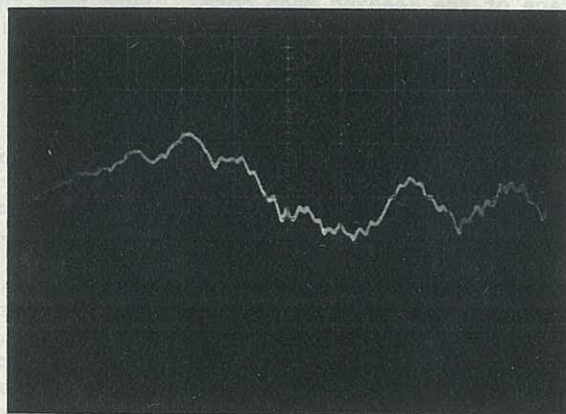
Figure 10 Correctly-expanded Mach 1.8 jet signature
(Jet exit centreline 0.18m from transducer)



(a) Shock-jet interaction photo T8



(b) Shock-jet interaction photo S7



(c) Shock-jet interaction photo V12

Figure 11 Random waveforms resulting from ballistic shock waves passing through correctly-expanded Mach 1.8 jets. (Distances identical to Figs. 9 and 10)

Due to the bow shock being bent forward by the jet, pressure signatures started 40-80 μ seconds earlier than those measured without a jet. The pressure perturbations were ~5 times larger for the supersonic nozzle than for the sonic nozzle. For the 114% expansion case, the pressure fluctuations of the Mach 1.8 jet were approximately the same size as the signature peak!

Bauer and Bagley (1970) presented 34 signatures out of the 630 interaction pressure signatures obtained. This paper has presented only 3 signatures out of

the total sample of 422, but all exhibit the same random variations from the basic N-wave (as did Bauer and Bagley's data) as flight test results in the presence of atmospheric turbulence.

4 CONCLUSIONS

It is a matter of interpretation of the schlieren photographs as to whether one attributes the shock 'rippling' to wavefront folding or to turbulent scattering of the shock front. The relatively composite shock fronts in Photos 2b and 2c indicate large-scale turbulence; whereas Mach 1.0 shock-jet interaction schlierens show small-scale turbulence.

Pressure signature data exhibited the same variability as bomber and fighter flight-test results. With the exception of 1% of the data at either extreme, the peak overpressure (using one of the two helium jets) was $\pm 50\%$ of the projectile peak over-pressure value. Eighty-three percent of the 422 data samples had the peak overpressure reduced when using a jet. The rise time to peak over-pressure was increased in 97% of the total sample. Thus, similar to flight-test results, rounded signatures occur more often than spiked ones.

5 ACKNOWLEDGMENTS

This paper is based upon experimental research undertaken in the Department of Mechanical Engineering, the University of Sydney as a Ph.D. candidate. The Dept of Transport (Air Group) funded this project from 1970-1973 as the Dept of Civil Aviation.

6 REFERENCES

BAUER, A.B. and BAGLEY, C.J. (1970). Sonic boom modeling investigation of topographic and atmospheric effects. U.S. Dept of Transport, Report FAA-NO-70-10.

BROWN, E.H. and CLIFFORD, S.F. (1976). On the attenuation of sound by turbulence. J. Acoust. Soc. Am., Vol. 60, No. 4, Oct. pp. 788-794.

BROWN, G.L. (1975, 1976). Private communication with author. Univ. of Adelaide, Mech. Eng.

CROW, S.C. (1969). Distortion of sonic bangs by atmospheric turbulence. J. Fluid Mech., Vol. 37, Pt. 3, pp. 529-563.

GEORGE, A.R. (1970). The effects of atmospheric inhomogeneities on sonic boom. Third Conf. on Sonic Boom Research, NASA SP-255, pp. 33-57.

GEORGE, A.R. and PLOTKIN, K.J. (1971). Propagation of sonic booms and other weak nonlinear waves through turbulence. Phys. Fluids, Vol. 14, pp. 548-554.

HALL, S-L. (1976). Refraction of the sonic-boom pressure signature by helium jets. Thesis (Ph.D.), Univ. of Sydney.

MAESTRELLO, L.; LIU, C.H.; GUNZBURGER, M. and TING, L. (1974). Sound propagation through a real jet flow field with scattering due to interaction with turbulence. AIAA Seventh Fluid and Plasma Dynamics Conf., Paper No. 74-551.

PIERCE, A.D. (1968). Spikes on sonic boom pressure waveforms. J. Acoust. Soc. Am., Vol. 44, No. 4, pp. 1052-1061.

PIERCE, A.D. (1971). Statistical theory of atmospheric turbulence effects on sonic boom rise times. J. Acoust. Soc. Am., Vol. 49, No. 3, pp. 906-924.

PIERCE, A.D. and MAGLIERI, D.J. (1972). Effects of atmospheric irregularities on sonic-boom propagation. J. Acoust. Soc. Am., Vol. 51, No. 2, pp. 702-721.

SANAI, M.; TOONG, T-Y. and PIERCE, A.D. (1976a). Ballistic range experiments on superbooms generated by refraction. J. Acoust. Soc. Am., Vol. 59, No. 3, pp. 513-519.

SANAI, M.; TOONG, T-Y. and PIERCE, A.D. (1976b). Ballistic range experiments on the superboom generated at increasing Mach numbers. J. Acoust. Soc. Am., Vol. 59, No. 3, pp. 520-524.